

MINISTRY OF
EDUCATION
AND TRAINING

VIETNAM ACADEMY OF
SCIENCE AND TECHNOLOGY

**GRADUATE UNIVERSITY OF SCIENCE AND
TECHNOLOGY**



NGUYEN DUONG BO

**MULTI COMPONENT CORRELATION EFFECT IN SOME
OPTICAL LATTICES**

DOCTORAL THESIS IN SCIENCE OF MATTER

Ha noi - 2025

The project is completed at Graduate University of Science and Technology - Vietnam Academy of Science and Technology.

Scientific Instructor: Assoc. Prof. Dr. Tran Minh Tien

Reviewer 1: ...

Reviewer 2: ...

Reviewer 3:

The thesis will be defended from the Board of marking doctor candidates' theses of the Graduate University of Science and Technology, that will be held in Graduate University of Science and Technology - Vietnam Academy of Science and Technology athour.....second, date.....month.....year

The thesis is able to be viewed in:

- Library of Graduate University of Science and Technology
- National Library of Vietnam

Novel contributions of the thesis

1. Mott transitions in three-component Falicov-Kimball model

Metal-insulator transitions are studied within a three-component Falicov-Kimball model, which mimics a mixture of one-component and two-component fermionic particles with local repulsive interactions in optical lattices. Within the model, the two-component fermionic particles are able to hop in the lattice, while the one-component fermionic particles are localized. The model is studied by using the dynamical mean-field theory with exact diagonalization. Its homogeneous solutions establish Mott transitions for both commensurate and incommensurate fillings between one-third and two-thirds. At commensurate one-third and two-thirds fillings, the Mott transition occurs for any density of hopping particles, while at incommensurate fillings, the Mott transition can occur only for density one-half of hopping particles. At half-filling, depending on the repulsive interactions, the reentrant effect of the Mott insulator is observed. As increasing local interaction of hopping particles, the first insulator-metal transition is continuous, whereas the second metal-insulator transition is discontinuous. The second metal-insulator transition crosses a finite region where both metallic and insulating phase coexist. At third-filling, the Mott transition is established only for strong repulsive interactions. A phase separation occurs together with the phase transition.

We consider a three-component FKM that describes a mixture of one-component heavy fermionic particles and two-component light fermionic particles loaded in an optical lattice. The heavy particles are

localized, whereas the light particles can hop in the lattice. Its Hamiltonian reads

$$H = -t \sum_{\langle i,j \rangle, \sigma} c_{i\sigma}^\dagger c_{j\sigma} + U_{cc} \sum_i c_{i\uparrow}^\dagger c_{i\uparrow} c_{i\downarrow}^\dagger c_{i\downarrow} \\ + E_f \sum_i f_i^\dagger f_i + U_{cf} \sum_i f_i^\dagger f_i c_{i\sigma}^\dagger c_{i\sigma},$$

where $c_{i\sigma}^\dagger$ ($c_{i\sigma}$) is the creation (annihilation) operator for a fermionic particle with hyperfine multiplet (or spin) σ at site i . σ takes two values ± 1 . t is the hopping parameter of the two-component fermionic particles, and we take into account only the hopping between nearest-neighbor sites. U_{cc} is the local Coulomb interaction between the two-component states of those particles. f_i^\dagger (f_i) is the creation (annihilation) operator for a one-component (or spinless) fermionic particle at site i . U_{cf} is the local Coulomb interaction between the two-component particles and one-component particles. The one-component particle does not move, and its energy level is E_f . E_f can also be considered as the chemical potential of the localized particles and controls the filling of the localized particles $n_f = \sum_i \langle f_i^\dagger f_i \rangle / N$, where N is the number of lattice sites. A common chemical potential μ is introduced to control the total particle filling $n_f = \sum_\sigma n_{c\sigma} + n_f$, where $n_{c\sigma} = \sum_i \langle c_{i\sigma}^\dagger c_{i\sigma} \rangle / N$.

Particles reads $G(\mathbf{k}, i\omega_n) = \frac{1}{i\omega_n + \mu - \varepsilon_{\mathbf{k}} \Sigma(i\omega_n)}$

where ω_n is the Matsubara frequency, $\varepsilon_{\mathbf{k}}$ is the dispersion of the two component particles, and $\Sigma(i\omega_n)$ is the self-energy.

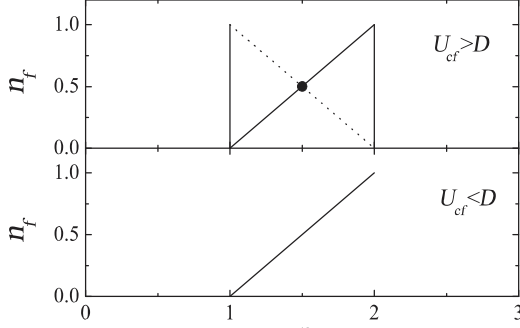


FIG. 1. Diagram of particle fillings for the MIT. The solid lines show the filling values of (n, n_f) at which the MIT can occur, and the dotted line shows the filling values of (n, n_f) for the occurrence of the inverse MIT. The black point indicates the filling value $(n = 3/2, n_f = 1/2)$ for the reentrant effect of the MIT

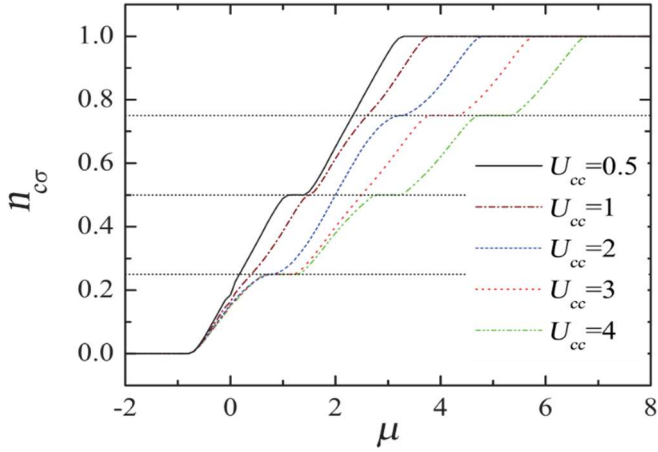


FIG. 2. The hopping particle filling $n_{c\sigma}$ as a function of the chemical potential μ at $n_f = 1/2$ for different values of U_{cc} and fixed $U_{cf} = 2$. The horizontal dotted lines show $n_{c\sigma} = 1/4$, $n_{c\sigma} = 1/2$, and $n_{c\sigma} = 3/4$ ($T = 0.01, D = 1$).

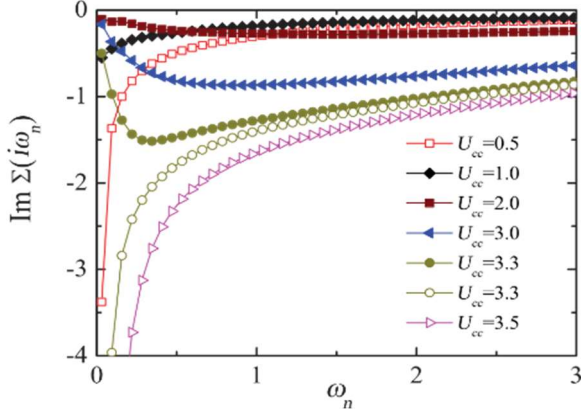


FIG. 3. The imaginary part of the light particle self-energy at half-filling for different values of U_{cc} and fixed $U_{cf} = 1.6$. ($T = 0.01, D = 1$).

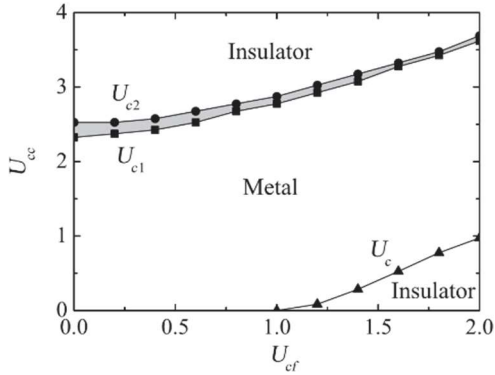


FIG. 4. Phase diagram at half-filling $n_{c\sigma} = n_f = 1/2$. In the grey area, both metallic and insulating phases coexist.

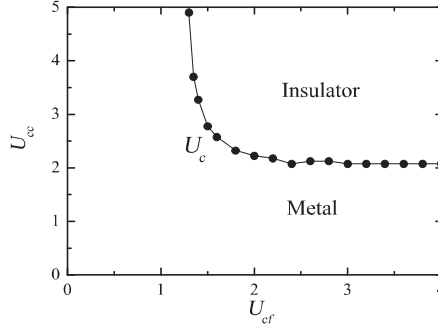


FIG. 4. Phase diagram for third-filling $n_{c\sigma} = n_f = 1/3$. ($T = 0.01$, $D = 1$).

2. Metal-insulator transition induced by mass imbalance in a three-component Hubbard model

We consider a three-component Hubbard model, the Hamiltonian of which reads

$$H = -\sum_{\langle i,j \rangle, \alpha} t_\alpha c_{i\alpha}^\dagger c_{j\alpha} + \frac{U}{2} \sum_{i, \alpha, \alpha'} t_\alpha c_{i\alpha}^\dagger c_{j\alpha \neq \alpha'},$$

Where $c_{i\alpha}^\dagger$ ($c_{i\alpha}$) is the creation (annihilation) operator for the fermionic particle with hyperfine multiplet α at site i . α takes three different values, for instance, $\alpha = 1, 2, 3$.

$n_{i\alpha} = c_{i\alpha}^\dagger c_{i\alpha}$ is the number operator of the α -component fermionic particles at site i . t_α is the hopping parameter of the α -

component fermionic particles. U is the local interaction between the three component states of particles. A common chemical potential μ is also introduced to control the total particle density $n = \sum_{i\alpha} \langle n_{i\alpha} \rangle / N$, where N is the number of lattice sites. The three-component Hubbard model can be realized by loading ultracold fermionic atoms with three hyperfine multiplets or fermion-fermion mixtures of different atomic species into optical lattices. However, in the Hamiltonian in Eq. the trapping potentials in the optical lattices are not considered.

The mass imbalance solely depends on the hopping parameters t_α . In the three-component Hubbard model, the mass imbalance actually means the difference of the hopping parameters. In optical lattices, the particle hopping is established by the particle tunneling between nearest- neighbor lattice potential wells. It can be tuned by the lattice potential amplitude V_α^{lat} and the recoil energy $E_{r\alpha}$ of each component state of particles

$$t_\alpha \approx \frac{4}{\sqrt{\pi}} E_{r\alpha} v_\alpha^{\frac{3}{4}} \exp(-2\sqrt{v_\alpha})$$

where $v_\alpha = \frac{V_\alpha^{\text{lat}}}{E_{r\alpha}}$. The recoil energy $E_{r\alpha} = \frac{k^2}{2m_\alpha}$, where k is the wave number of the laser forming the optical lattice, and m_α is the mass of the α -component particles. The lattice potential amplitude V_α^{lat} can be different for different hyperfine states of particles. As a result, the hopping parameters can also be different even for the hyperfine states of the same particles with identical masses. In the following, we will consider the hopping imbalance $t_1 \neq t_2 = t_3$. This case can be interpreted

as a fermion-fermion mixture of two different particle species. One species is particles with a single hyperfine state ($\alpha = 1$), while the other is particles with two hyperfine states ($\alpha = 2,3$). Such mixture can be realized by loading fermion atoms ^{40}K and ^6Li , or of light atoms ^6Li or ^{40}K with heavy fermion isotopes of Sr or Yb, into optical lattices. We parametrize the hopping amplitudes by

$$t = \frac{t_1 + t_2}{2}$$

$$\Delta t = \frac{t_2 - t_1}{t_1 + t_2}.$$

t is the average hopping amplitude of two particle species, and Δt describes the mass imbalance between them.

It is clear that $-1 \leq \Delta t \leq 1$. $\Delta t = \pm 1$ are the extreme mass imbalance, where one particle species is extremely heavy and localized

The Green's function of the α -component particles reads

$$G_\alpha(\mathbf{k}, i\omega_n) = \frac{1}{i\omega_n + \mu + t_\alpha \varepsilon_{\mathbf{k}} - \Sigma_\alpha(i\omega_n)},$$

where ω_n is the Matsubara frequency, $\varepsilon_{\mathbf{k}} = \sum_{\langle i,j \rangle} \exp[i\mathbf{k} \cdot$

$(\mathbf{r}_i - \mathbf{r}_j)]$ is the lattice structure factor, and $\Sigma_\alpha(i\omega_n)$ is the self-energy.

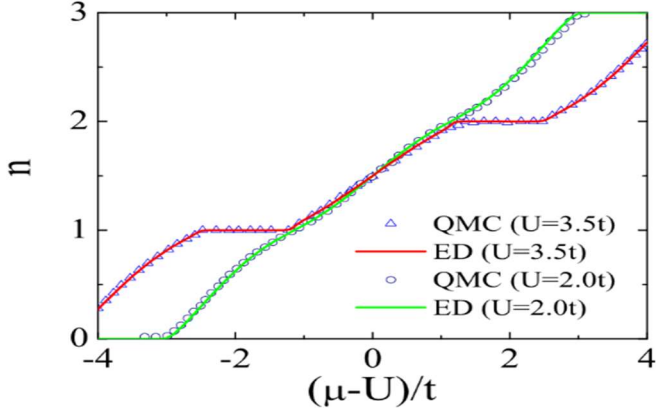


FIG. 1. The total particle density n , calculated by DMFT+ED (lines) and by DMFT+QMC (symbols), as a function of the chemical potential μ for different values of interaction U in the balanced mass case $\Delta t = 0$ ($T = 0.025t$). The DMFT+QMC results are reproduced from Ref.

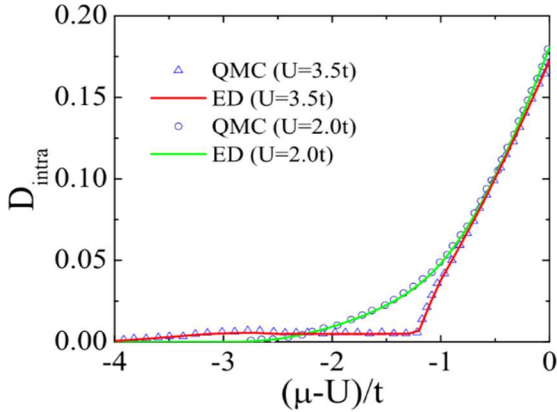


FIG. 2. (Color online) The double occupancy as a function of the chemical potential μ , calculated by DMFT+ED (lines) and by DMFT+QMC (symbols) for different values of interaction U in the

balanced mass case $\Delta t = 0$ ($T = 0.025t$). The DMFT+QMC results are reproduced from Ref.

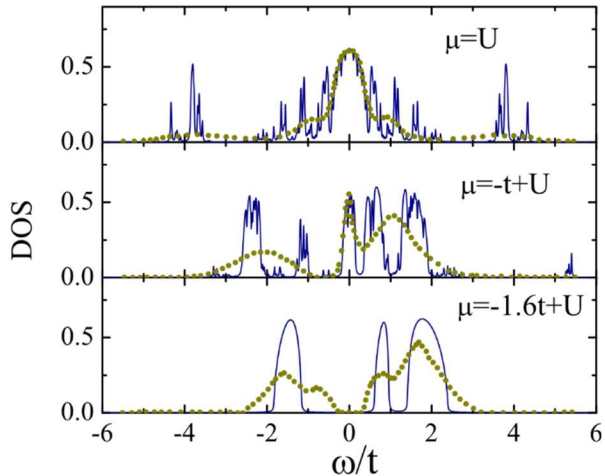


FIG. 3. (Color online) The density of states (DOS), calculated by DMFT+ED (lines) and by DMFT+QMC (symbols) for different chemical potentials μ in the balanced mass case $\Delta t = 0$ ($U = 3t$, $T = 0.05t$). The DMFT+QMC results are reproduced from Ref.

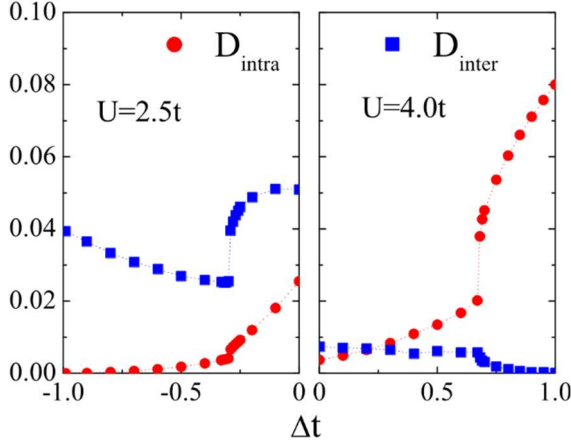


FIG. 4. (Color online) The intraspecies double occupancy D_{intra} (red filled circles) and the interspecies double occupancy D_{inter} (blue filled squares) at fixed total density $n = 1$ ($T = 0.02t$). The left panel plots the region of $\Delta t < 0$ ($U = 2.5t$), while the right panel plots the region of $\Delta t > 0$ ($U = 4t$).

3. COMPETITION BETWEEN THE SOFT GAP AND THE MOLECULAR KONDO SINGLETs IN FLAT-BAND LATTICES

One of the simplest flat-band lattices is the Lieb lattice. The Lieb lattice is a square lattice with additional sites at the middle of every square edge (see Fig. 1). The Lieb lattice has attracted research attention since the discovery of high-temperature superconductivity because it is the basic structure of CuO_2 plane of the cuprate superconductors. The Lieb lattice can be also artificially made by optical lattices, ultracold atoms, and molecular design.

We consider a magnetic impurity, which is placed at a corner site (A site in Fig. 1), and hybridizes with conduction electrons at site A as well as at the nearest neighbor sites. The Hamiltonian of the model reads

$$\begin{aligned}
H = & -t \sum_{\langle i,j \rangle, \sigma} c_{i\sigma}^\dagger c_{j\sigma} + \varepsilon \sum_{\sigma} n_{A\sigma}^f + U n_{A\uparrow}^f n_{A\downarrow}^f \\
& + V_0 \sum_{\sigma} c_{A\sigma}^\dagger f_{A\sigma} + \\
& H.c. + V_1 \sum_{i(A), \sigma} c_{A\sigma}^\dagger f_{A\sigma} + H.c
\end{aligned}$$

where $c_{i\sigma}^\dagger c_{i\sigma}$ is the creation (annihilation) operator of conduction electron at site i with spin σ . t is the hopping parameter. Here we take into account only the nearest neighbor hopping

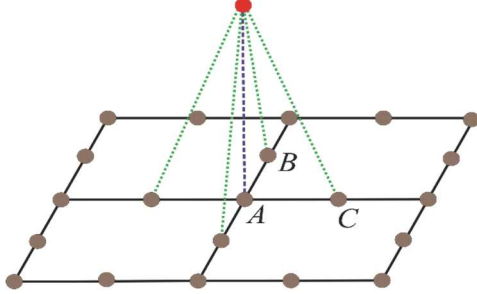


Fig. 1. The Lieb lattice structure. The magnetic impurity (red dot) is hybridized with conduction electrons at the corner site (A site) as well as at the edge center sites, surrounding the corner site (B and C sites).

of conduction electrons. $f_{A\sigma}^\dagger$ ($f_{A\sigma}$) is the creation (annihilation) operator of impurity with spin σ at site A . $n_{A\sigma}^f = f_{A\sigma}^\dagger f_{A\sigma}$ is the number operator of the magnetic impurity. ε is the energy level of the magnetic impurity, and U is the Coulomb interaction of electrons at the impurity site. The magnetic impurity hybridizes with conduction electrons at site A by strength V_0 , and with conduction electrons at nearest neighbor sites by strength V_1 . When $V_1 = 0$, Hamiltonian in Eq. (1) reduces to the one of the soft-gap Kondo problem [6, 7]. When $V_0 = 0$, Hamiltonian in Eq. (1) basically describes the molecular Kondo problem [2]. For finite hybridizations V_0 , V_1 , Hamiltonian in Eq. (1) would describe the competition between the soft-gap and the molecular Kondo effect, which may occur in the system. We parameterize these hybridization strengths by

$$V_0 = \frac{1}{2}(1 + \alpha)V,$$

$$V_1 = \frac{1}{2}(1 - \alpha)V.$$

When $\alpha = 1$, $V_0 = V$ and $V_1 = 0$. When $\alpha = -1$, $V_0 = 0$ and $V_1 = V$. When $-1 < \alpha < 1$, both V_0 and V_1 are finite. The parameter α describes the difference relation between V_0 and V_1 , while V is the total hybridization strength.

The Kondo problem totally depends on the hybridization function

$$\Delta(\omega) = \frac{1}{N} \sum_k \Gamma_k^\dagger [\omega - h_0(k)]^{-1} \Gamma_k,$$

Where $\Gamma_k^\dagger = (V_0, 2V_1 \cos(k_x/2), 2V_1 \cos(k_y/2))$, and $h_0(k)$ is the Bloch Hamiltonian of conduction electrons

$$h_0(k) = \begin{pmatrix} 0 & -2t \cos\left(\frac{k_x}{2}\right) & -2t \cos\left(\frac{k_y}{2}\right) \\ -2t \cos\left(\frac{k_x}{2}\right) & 0 & 0 \\ -2t \cos\left(\frac{k_y}{2}\right) & 0 & 0 \end{pmatrix}.$$

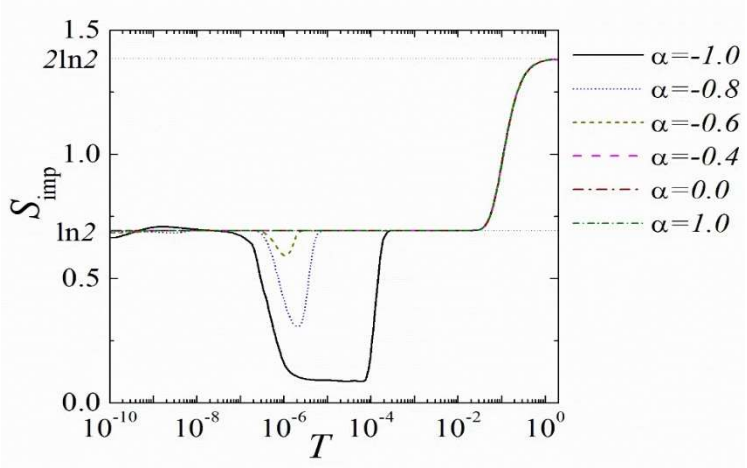


Fig. 2. The impurity entropy as a function of temperature for different values of α . $U=0.5$, $\Gamma=0.001$, $\eta=10^{-9}$.

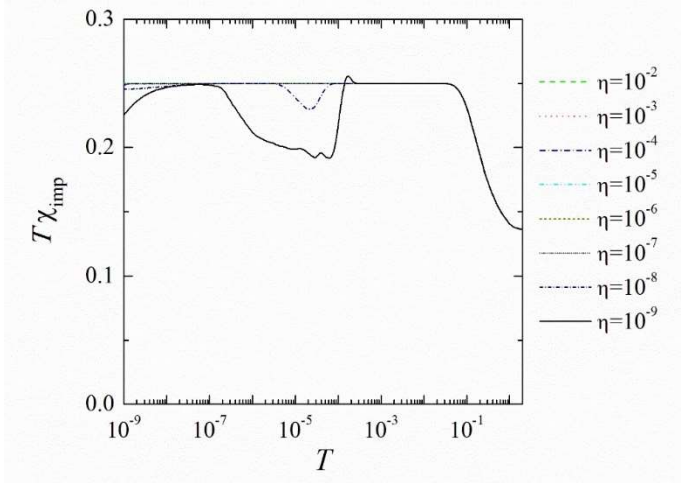


Fig. 3. The impurity spin susceptibility as a function of temperature for different values of η . $U=0.5$, $\Gamma=0.001$, $\alpha=-1$.

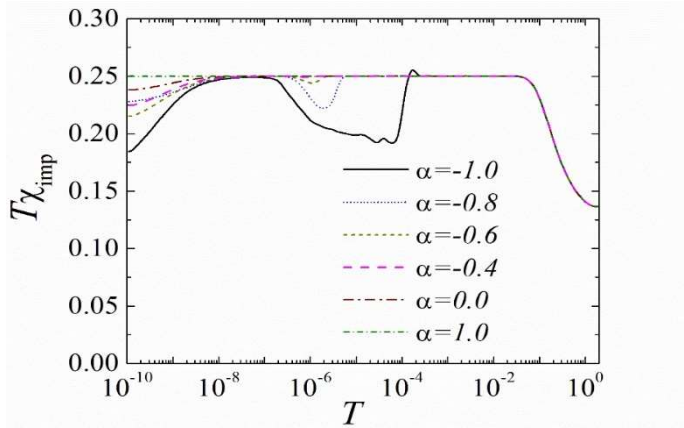


Fig. 4. The impurity spin susceptibility as a function of temperature for different values of α . $U= 0.5$, $\Gamma= 0.001$, $\eta= 10^{-9}$.

4. Selective Kondo strong coupling in magnetic impurity flat-band lattices

In this thesis we investigate a possibility of the selective Kondo strong coupling in the magnetic impurity flat-band lattices. One of the simplest flat-band lattices is the Lieb lattice, where the electron structure of the tight-binding model features both the band flatness and the Dirac linear dispersion at low energy. With the such electron structure the Lieb lattice allows us to study the competition between the molecular and the soft-gap Kondo strong couplings. As a result of the competition a selective Kondo strong coupling may occur. For the purpose we study the periodic Anderson model (PAM) on the Lieb lattice. The model essentially describes the hybridization between the magnetic impurities and conduction electrons of both the flat and the Dirac-cone bands. The competition between the molecular and the soft-gap Kondo strong couplings could emerge at strong electron correlations. We will adopt the slave-boson mean-field approximation to study the competition. The slaveboson mean-field approximation is simple, and it can well describe the essential features of the strong coupling(SC) and local moment (LM) regimes in the PAM. Recently, the slave-boson mean-field approximation was

also used to study the interlay between the Kondo effect and topology. We find very rich phase diagrams depending on the impurity parameters. In general, the full local moment (FLM) regime, where all magnetic impurities are decoupled from conduction electrons, appears at high temperature. At low temperature and strong hybridization, the full strong coupling (FSC) regime, where all magnetic moments form the Kondo singlets with conduction electrons, exists. Between the FLM and the FSC regimes, various selective Kondo strong coupling regimes occur. The stability of the selective Kondo strong coupling is essentially due to the low-energy properties of conduction bands, which hybridize with magnetic impurities. The obtained results predict the selective Kondo strong coupling in heavy-fermion materials, topological semimetals, systems with nonuniform lattice coordination number, where either a flat band exists or the bands of conduction electrons have qualitatively different low-energy properties.

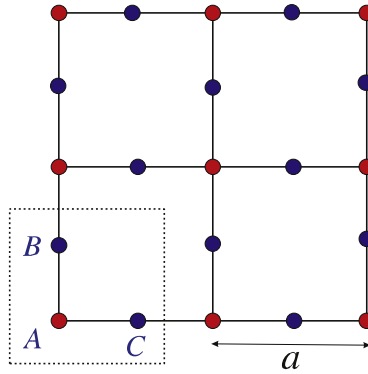


Fig. 1. The Lieb lattice structure.

The present thesis is organized as follows. In Section 2 we describe the PAM on the Lieb lattice. In this section we also present the slave-boson approach and its mean-field approximation. The numerical results for depleted lattices are presented in Section 3, and in Section 4 the phase diagrams for uniform hybridizations are presented. Finally, discussion and conclusion are presented in Section

The PAM is a lattice generation of the single impurity Anderson model. It describes a lattice of localized electrons hybridized with conduction electrons. The PAM is a suitable model for studying heavy fermion compounds. Its Hamiltonian reads

$$H = -t \sum_{\langle i,j \rangle \sigma} c_{i\sigma}^\dagger c_{j\sigma} + \sum_{i\sigma} \varepsilon_i f_{i\sigma}^\dagger f_{i\sigma} + U \sum_i n_{fi\uparrow} n_{fi\downarrow} + \sum_{i\sigma} V_i c_{i\sigma}^\dagger f_{i\sigma} + H.c.,$$

where $c_{i\sigma}^\dagger (c_{i\sigma})$ is the creation (annihilation) operator for conduction electron with spin σ at lattice site i . t is the nearest neighbor hopping parameter. $f_{i\sigma}^\dagger (f_{i\sigma})$ represents the creation (annihilation) operator for the magnetic impurity with spin σ at site i . ε_i is the energy level of the magnetic impurity. $f_{i\sigma}^\dagger f_{i\sigma}$ is the impurity number at site i . U is local Coulomb interaction of impurity electrons. $n_{fi\sigma}$ operator.

Some results.

Fig. 2 . Depleted lattice with $V_A \equiv V$, and $V_B = V_C = 0$. Left panel: Phase diagram for different values of ε_A (the solid, dotted and dashed lines for $\varepsilon_A = -0.05, -0.1$, and -0.2 , respectively). Right panel: LDOS of conduction electrons (solid line) and of magnetic impurities (dotted line) at A site in the SC phase for $V^2 = 0.25$, and $\varepsilon_A = -0.1$ ($T = 0.1$). The broadening parameter $\eta = 10^{-4}$.

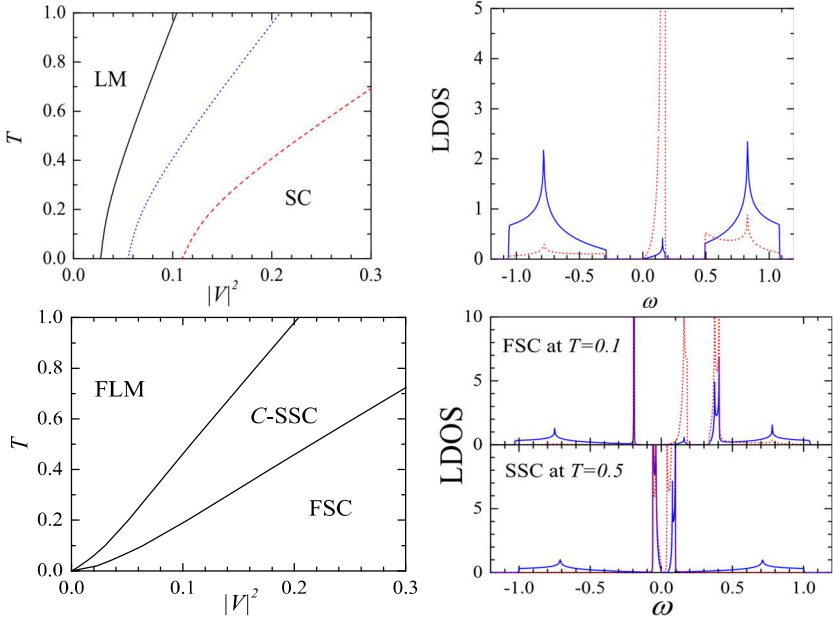


Fig. 3. Depleted lattice with $V_A = 0$ and $V_B = V_C \equiv V$. Left panel: Phase diagram for $\varepsilon_B = -0.2$, $\varepsilon_C = -0.1$. Right panel: LDOS of conduction electrons (solid line) and of magnetic impurities (dotted line) at the C site in the FSC and the SSC phases for $V^2 = 0.15$, $\varepsilon_B = -0.2$, $\varepsilon_C = -0.1$. The broadening parameter $\eta = 10^{-4}$.

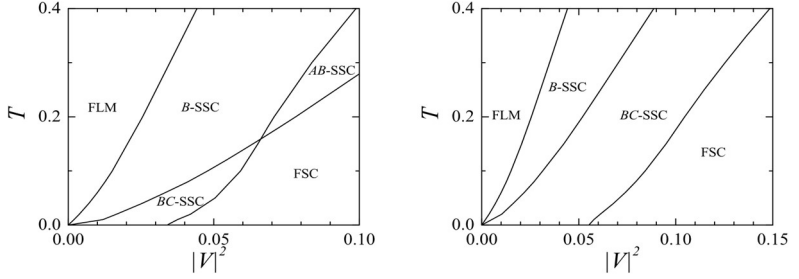


Fig. 4. Phase diagram for uniform hybridizations $V_A = V_B = V_C = V$. Left panel: case $\varepsilon_A = -0.1$, $\varepsilon_B = -0.05$, $\varepsilon_C = -0.15$. Right panel: case $\varepsilon_A = -0.15$, $\varepsilon_B = -0.05$, $\varepsilon_C = -0.1$.

LIST OF THE AUTHOR'S WORKS

I. Publication of results used in the thesis

International Magazin:

1. Duong-Bo Nguyen and Minh-Tien Tran, *Mott transitions in three-component Falicov-Kimball model*, Physical Review B, 2013, 87, 045125.
2. Duong-Bo Nguyen, Duy-Khuong Phung, Van-Nham Phan, and Minh-Tien Tran, *Metal-insulator transition induced by mass imbalance in a three-component Hubbard model*, Physical Review B, 2015, 91, 115140.
3. Duong-Bo Nguyen, Thanh-Mai Thi Tran, Thuy Thi Nguyen, Minh-Tien Tran, *Selective Kondo strong coupling in magnetic impurity flat-band lattices*, Annals of Physics, 2019, 400, 9.

National magazine

1. Duong-Bo Nguyen, Hong-Son Nguyen and Minh-Tien Tran, *Competition between the soft gap the molecular Kondo singlets in flat-band latties*, Communications in Physics, 2018, 28, 361.